

Coalescence and interface diffusion in linear CdTe/CdSe/CdTe heterojunction nanorods

Bonil Koo and Brian A. Korgel*

Department of Chemical Engineering, Center for Nano- and Molecular Science and Technology, and Texas Materials Institute, The University of Texas at Austin, Austin, Texas 78712-1062

* Corresponding author. E-mail: korgel@che.utexas.edu. Tel: (512) 471-5633. Fax: (512) 471-7060.

Supporting Information

Experimental Details

Chemicals. Cadmium oxide (CdO, 99.5%), tellurium (Te, 99.8%), tributylphosphine (TBP, 97%), and toluene (99.8%) were purchased and used as received from Aldrich. n-Tetradecylphosphonic acid (TDPA, 97%) was purchased from Alfa Aesar. Tri-n-octylphosphine (TOP, 97%), trioctylphosphine oxide (TOPO, 99%), and selenium (Se, 99.99%) were purchased from STREM.

Synthesis of CdTe/CdSe/CdTe heterojunction nanorods. A Cd-TDPA complex¹ was prepared by adding 0.963 g of CdO (7.5 mmol) and 4.185 g of TDPA (15 mmol) to 3 g of TOPO and degassing for one hour through pulling vacuum in the Schlenk line. The mixture was heated to 300 °C under nitrogen. It kept aged for 10 minutes until it turned optically clear, indicating that the Cd-TDPA complex formed. Subsequently, the clear Cd-TDPA solution was cooled at room temperature to be solidified and aged for more than 24 hr. This Cd-TDPA complex is

important for making the CdSe nanorods, as its stability leads to distinct particle nucleation followed by slow controlled growth, which is necessary for nanorod formation.²

A mixture of 3.48 g of Cd-TDPA complex (3.2 mmol of Cd) and 4.65 g of TOPO was degassed in the reaction flask for one hour and then heated to 320 °C under nitrogen. A selenium precursor reactant solution was prepared by dissolving 0.126 g of Se (1.6 mmol) in a mixture of 0.468 mL of TBP, 3.482 mL of TOP, and 0.694 mL of toluene at 120 °C. The tellurium reactant solution was made under the same condition except with an increased amount (5 mL) of TOP to lower the solution viscosity for easy injection through a syringe pump. The selenium precursor was rapidly injected into the mixture of Cd-TDPA and TOPO at 320 °C. The temperature was then immediately decreased to 250 °C. This temperature decrease promotes the formation of relatively high aspect ratio CdSe nanorods.¹ After heating for 30 minutes, the reaction solution was returned to 300 °C and then the tellurium precursor was injected by syringe pump for 7.5 minutes at a rate of 48 mL/hr, which yields CdTe/CdSe/CdTe heterojunction nanorods.²

Nanorod aging. After Te injection from the syringe pump was complete, the CdTe/CdSe/CdTe heterojunction nanorods were stirred in solution for 30 hr at 300 °C. Nanorods were removed from solution at different times in ~0.5 mL aliquots for characterization. Prior to characterization, the nanorods in each aliquot were purified by precipitation with excess ethanol, followed by centrifugation. The precipitated nanorods were redispersed chloroform or toluene for characterization.

Materials Characterization. Low resolution transmission electron microscopy (LRTEM) images were acquired using a Phillips EM280 microscope operated at an accelerating voltage of 80 kV. High resolution electron transmission microscopy (HRTEM) images were obtained using a JEOL 2010F microscope equipped with a field emission gun operated at 200 kV. TEM

samples were prepared by drop-casting dilute solutions of nanorods from toluene onto a carbon-coated copper TEM grid (200-mesh, Ladd Research).

Energy dispersive X-ray spectroscopy (EDS) mapping was performed on an FEI TECNAI G2 F20 X-TWIN microscope in scanning transmission electron microscopy (STEM) mode at an accelerating voltage of 200 kV. Drift corrected spectrum profiles were obtained by initially selecting a reference area in STEM image and regulating the scanning direction not to stray from the reference area. The electron beam was focused to a spot size of ~0.5 nm in diameter. During EDS mapping, the dwell time was 1000 ms at a given position and the profile size was 400 positions per nanorod. The spatial resolution of this technique is ~1 nm.

X-ray diffraction (XRD) was performed on a Bruker-Nonius D8 Advance powder diffractometer with Cu K α radiation ($\lambda = 1.54 \text{ \AA}$). Nanorods were evaporated from toluene onto quartz substrates and dried to make thick films (~200 μm). Diffraction patterns were obtained at a scan rate of 12 deg / min in 0.01 deg increments for 12 hr, rotating the sample at 15 deg / min.

UV-visible absorbance spectra were collected on a Varian Cary 5000 Scan spectrophotometer and photoluminescence (PL) spectra were recorded using a Fluorolog-3 fluorometer with a 450W Xe source. The absorbance and PL spectra were measured at room temperature with nanocrystals dispersed in toluene. PL measurements were taken with nanorod concentrations adjusted so that the at the first exciton peak wavelength—which was also the excitation wavelength—was 0.1.

X-ray diffraction (XRD).

Figure S1 shows XRD data for CdTe/CdSe/CdTe nanorods as-synthesized and aged in solution. The broadened peaks in the range of $2\theta = 40\sim 50^\circ$ that appear after 10 minutes of aging

in solution at 300°C indicate that there is relatively significant Te/Se interdiffusion across the heterojunction. After 1 hour of aging in solution, the XRD peaks have broadened and shifted to lower angle, indicating that a significant amount of CdSe/CdTe alloying due to Se-Te interdiffusion across the heterojunctions has occurred. After 30 hours of aging, the nanorods have formed a CdSe_{0.4}Te_{0.6} alloy. Figure S2 shows XRD data for the CdTe/CdSe/CdTe nanorods that were redispersed at 300°C after first purifying them to try to remove all residual reactants and then after 30 hours of aging. The XRD pattern corresponds to a CdSe_{0.48}Te_{0.52} alloy.

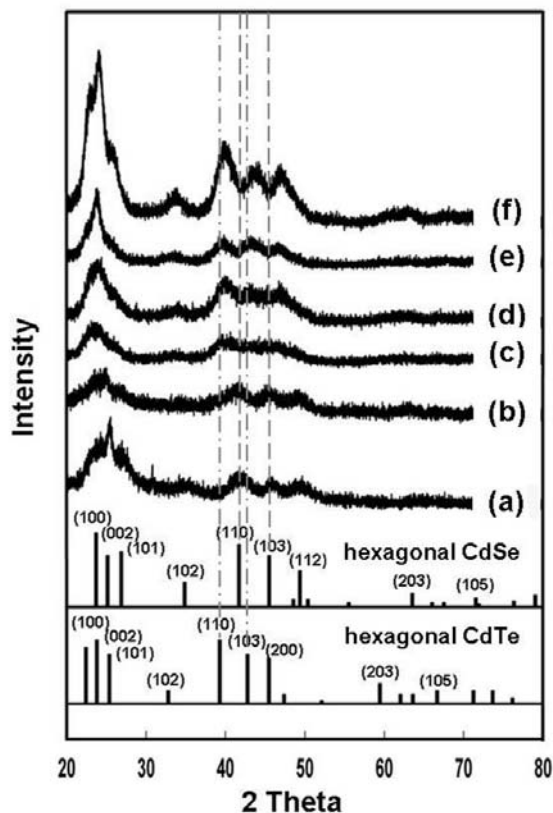


Figure S1. X-ray diffraction (XRD) of (a) CdSe nanorods prior to CdTe addition and CdTe/CdSe/CdTe heterojunction nanorods (b) immediately following CdTe deposition and after aging in solution at 300 °C for (c) 10min, (d) 1 hr, (e) 7 hr, and (f) 30 hr. The broadened peaks in the range of $2\theta = 40\sim 50^\circ$ in (c) result from the beginning of Te/Se interdiffusion. The XRD

pattern (f) corresponds to $\text{CdSe}_{0.4}\text{Te}_{0.6}$ alloy with hexagonal crystal structure: $d_{002} = 3.66 \text{ \AA}$, $d_{110} = 2.24 \text{ \AA}$, giving $a_{\text{CdSe}_x\text{Te}_{1-x}} = 4.48 \text{ \AA}$, $c_{\text{CdSe}_x\text{Te}_{1-x}} = 7.3 \text{ \AA}$, which corresponds to the lattice parameters expected for $\text{CdSe}_{0.4}\text{Te}_{0.6}$.

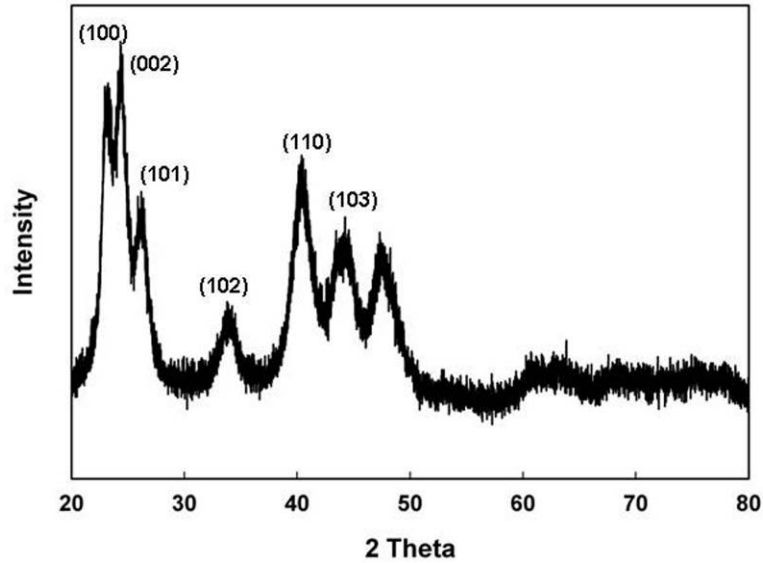


Figure S2. XRD of the coalesced nanorods imaged by TEM in Figure 3f, which have been aged in solution at 300°C for 30 hr after an initial purification step. The lattice constants of $a = 4.4 \text{ \AA}$ and $c = 7.26 \text{ \AA}$ determined from the (002) and (110) peak positions, $d_{002} = 3.63 \text{ \AA}$ and $d_{110} = 2.20 \text{ \AA}$ correspond to a final alloy composition of $\text{CdSe}_{0.48}\text{Te}_{0.52}$, which is consistent with the volume change measured and plotted in Figure 4 of the main body of the paper.

Nanorod Length and Diameter Histograms.

Figure S3 shows histograms of nanorod length and diameter distributions determined from TEM measurements, corresponding to the nanorod samples shown in Figure 1 in the main body of the paper.

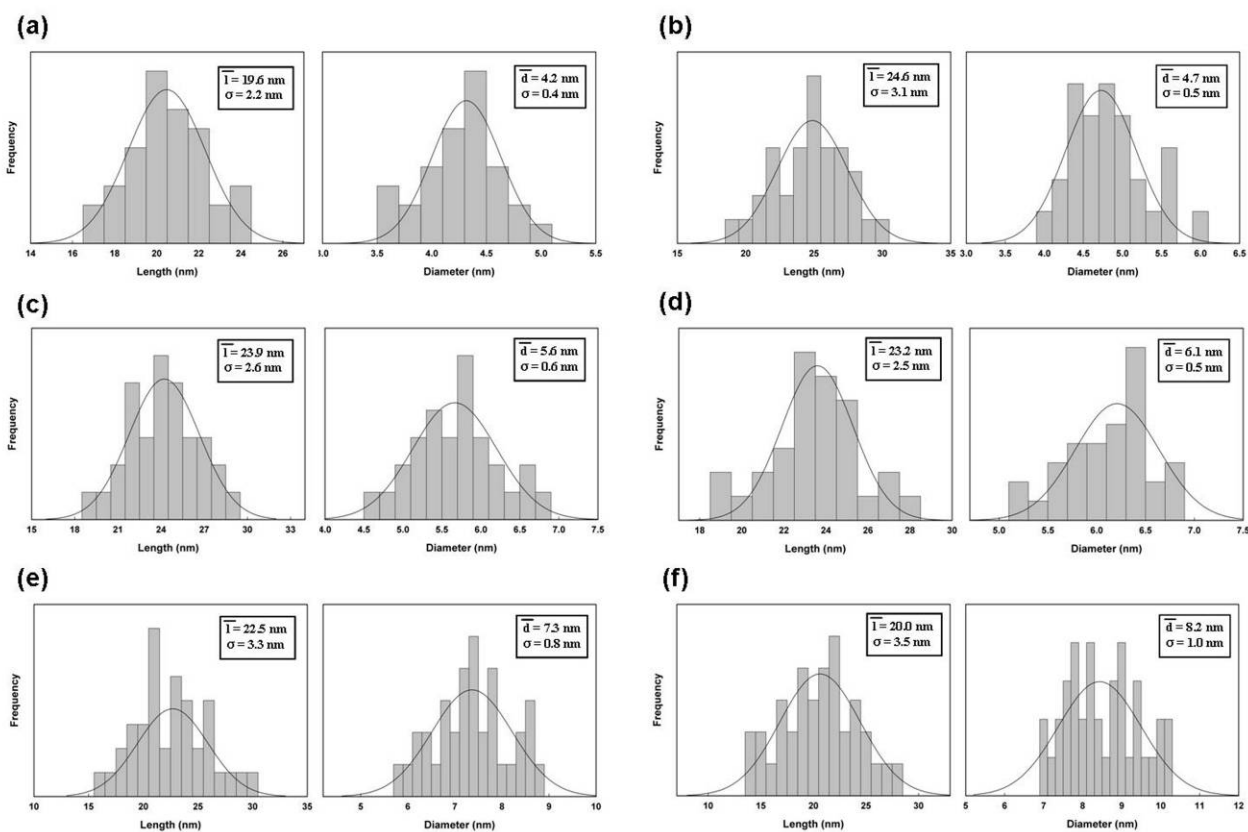


Figure S3. Histograms of length and diameter of (a) CdSe nanorods and the CdTe/CdSe/CdTe heterojunction nanorods after (b) initial CdTe deposition and then stirring in solution at 300 °C for (c) 10 min, (d) 1 hr, (e) 7 hr, and (f) 30 hr. The nanorod dimensions were determined from TEM images. The histograms correspond to the nanorod samples imaged in Figure 1 in the main body of the paper.

Derivation of the continuum viscous flow model for nanorod coalescence.³

The nanorods are assumed to have a cylindrical shape with radius r , and length L , as shown in Figure S4, with volume V , and surface area A :

$$V = \pi r^2 \times L \quad (1)$$

$$A = (2\pi r^2) + (2\pi rL) \quad (2)$$

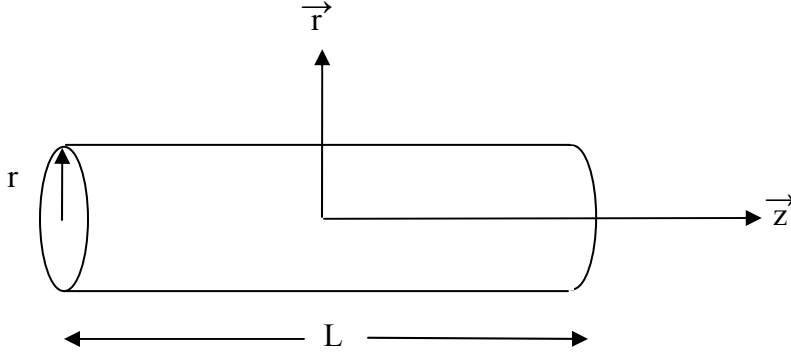


Figure S4. Cylindrical model for a nanorod.

As the nanorod coalesces to a sphere, its surface energy E , decreases and

$$\frac{dE}{dt} = -\sigma \frac{dA}{dt} \quad (3)$$

Since $A = (2\pi r^2) + (2\pi rL)$,

$$\frac{dA}{dt} = \left(4\pi r \frac{dr}{dt}\right) + \left(2\pi L \frac{dr}{dt}\right) + \left(2\pi r \frac{dL}{dt}\right). \quad (4)$$

Since the volume of the nanorod does not change as it coalesces, dL/dt and dr/dt are related:

$$\frac{dV}{dt} = 0 = 2\pi rL \frac{dr}{dt} + \pi r^2 \frac{dL}{dt} \quad (5)$$

so that

$$\frac{dr}{dt} = -\frac{1}{2} \left(\frac{r}{L} \right) \frac{dL}{dt} . \quad (6)$$

Plugging Eqn (9) into Eqn (3):

$$-\sigma \frac{dA}{dt} = -\sigma \left[\left(-\frac{2\pi r^2}{L} \frac{dL}{dt} \right) + \left(-\pi r \frac{dL}{dt} \right) + \left(2\pi r \frac{dL}{dt} \right) \right] = -\sigma \pi r \left[1 - 2 \left(\frac{r}{L} \right) \right] \frac{dL}{dt} \quad (7)$$

This energy change is dissipated by molecular motions in the nanorod. Assuming that viscous energy losses dissipate the change in surface energy, then⁵

$$-\sigma \frac{dA}{dt} \approx 3\eta \alpha^2 \pi r^2 L \quad (8)$$

where η is the viscosity and α is a linear compression coefficient over time:

$$\alpha \equiv -2 \left(\frac{1}{L} \right) \frac{dL}{dt} . \quad (9)$$

It follows from

$$3\eta \alpha^2 \pi r^2 L = -\sigma \pi r \left[1 - 2 \left(\frac{r}{L} \right) \right] \frac{dL}{dt} , \quad (10)$$

that

$$\alpha = \frac{\sigma}{2\eta r} \left(1 - 2 \left(\frac{r}{L} \right) \right) = -2 \left(\frac{1}{L} \right) \frac{dL}{dt} , \quad (11)$$

so that

$$\frac{dL}{dt} = -\alpha \frac{L}{2} = -\frac{\sigma}{3\eta r} \left(1 - 2 \left(\frac{r}{L} \right) \right) L . \quad (12)$$

Eqn (12) is the instantaneous coalescence rate for a rod of length L and radius r . The length L , of a coalescing nanorod and the coalescence time can be determined by integration of Eqn (12) and assuming a cylindrical geometry such that $r = \sqrt{V/\pi L}$:

$$t = -\frac{12\eta}{\sigma} \int_{L_0}^L \left(\sqrt{\frac{\pi}{V}} L^{3/2} - 2 \right)^{-1} dL \quad (13)$$

L_0 is the initial length of the nanorod at $t=0$. Similarly, the coalescence time and the nanorod radius are related, where R_0 is the initial radius:

$$t = \frac{24\eta}{\sigma} \int_{R_0}^R \left(1 - \frac{2\pi r^3}{V} \right)^{-1} dr \quad (14)$$

Figure S5 shows Eqns (13) and (14) plotted as a function of different values of σ/η and compared to the experimental data from Figure 5 in the main body of the paper. The instantaneous coalescence rate, dL/dt (and dr/dt), decreases as the nanorod aspect ratio decreases towards 1. The coalescence rate is slower for higher η (corresponding to lower D) and lower σ .

A relationship between η and D is needed to compare the coalescence rate predicted by Eqns (13) and (14) to the measured coalescence rates. The Eyring equation provides such a relationship for a fluid,⁶

$$\eta = \frac{kT}{a_0 D} \quad (15)$$

where a_0 is an interatomic spacing (e.g. bond length of CdTe = 2.8×10^{-10} m) and D is the diffusion coefficient. The dashed lines in Figure S5 show the predicted coalescence rate predicted from Eqns (13) and (14) using Eqn (15) to relate D and η . However, since the growth temperature is well below the melting points of CdSe and CdTe, use of the Eyring equation gives only a lower bound for η , corresponding to an upper bound for the nanorod coalescence rate. For an elastic solid with nanoscale crystal domain size—as is the case for the nanorods here—

Herring showed that a “diffusional viscosity” can be determined from D and the grain size (in this case, the nanorod radius R):⁷

$$\eta = \frac{kTR^2}{4\Omega_0 D} \quad (16)$$

where Ω_0 is the atomic volume. Using this expression, η is almost 2 orders of magnitude higher than η estimated using Eyring’s equation for a fluid. Plots of the coalescence rates calculated using Eqns (13) and (14) and (16) are given in Figure 5 in the main body of the paper.

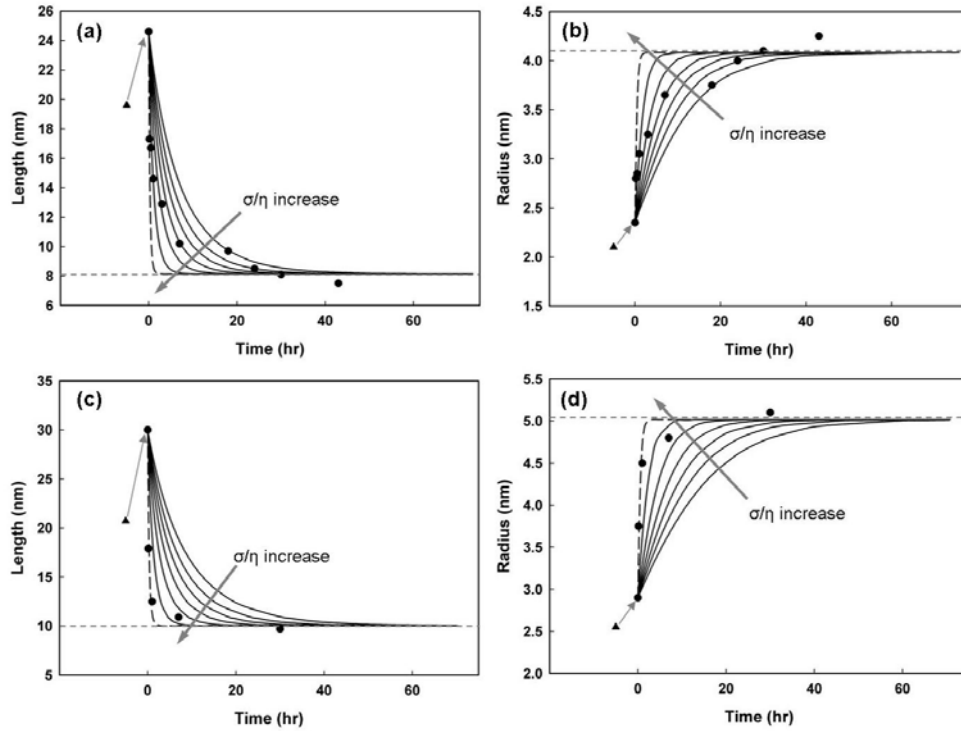


Figure S5. Comparison between the (●) measured (a,c) length and (b,d) radius of nanorods aged in solution at 300°C and the coalescence rates (—) predicted by Eqns (13) and (14). The data correspond to the data in Figure 5 in the main body of the paper. The flat dashed line in each figure corresponds to the length and radius of the nanorods after they have coalesced.

EDS mapping data and Te diffusion length determination.

Figures S6 and S7 show EDS mapping data for several CdTe/CdSe/CdTe nanorods after different aging times in solution at 300°C. Figure S6 shows examples of the Cd, Se and Te profiles of four different nanorods that were isolated and mapped after different aging times. The Se and Te profiles are relatively flat after 7 hours of aging, although there is a slight excess of Te still observable at the tips of the nanorods, as in Figure S6(d) in the upper right and lower left panels. Two of the nanorods mapped after 30 hr of aging also have a slight excess of Te at their tips, which is the result of continued Te deposition in solution from remaining reactant, as discussed in the body of the paper. To determine the Te diffusion length in the nanorods after different aging times, the edge of the Te profile in the center of each nanorod was estimated as illustrated in Figure S7. An exact determination of the Te edge was complicated by the fact that the Te composition could not be monitored in one nanorod as it aged in solution and additionally that the average nanorod length decreased as a result of coalescence. Nonetheless, the edge of the heterojunction interface could be estimated with reasonable accuracy by examining the Te profiles in several different nanorods and averaging their diffusion lengths. Figure S8 shows additional plots of the Se to Cd and Te to Cd ratios determined from the EDS maps to further illustrate how the diffusion length was determined. These plots reveal that significant Se and Te interdiffusion has occurred after 1 hour of aging in solution and that after 7 hours of aging the Se and Te concentrations have become uniform.

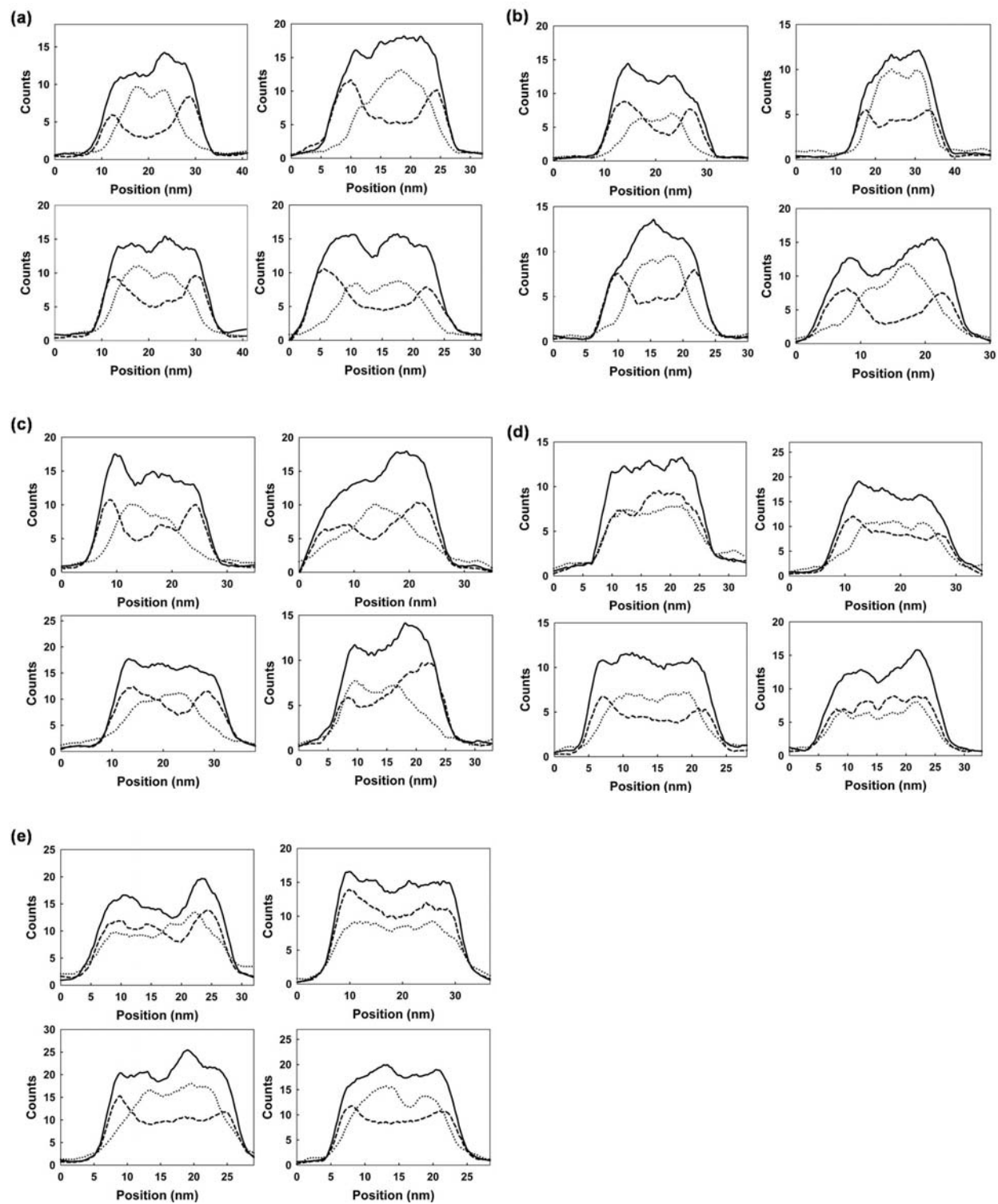


Figure S6. Nanobeam EDS maps of Cd (—), Te (---) and Se (·····) compositional profiles along the lengths of individual CdTe/CdSe/CdTe nanorods: (a) immediately after synthesis and after aging in solution at 300°C for (b) 10 min, (c) 1 hr, (d) 7 hr, and (e) 30 hr.

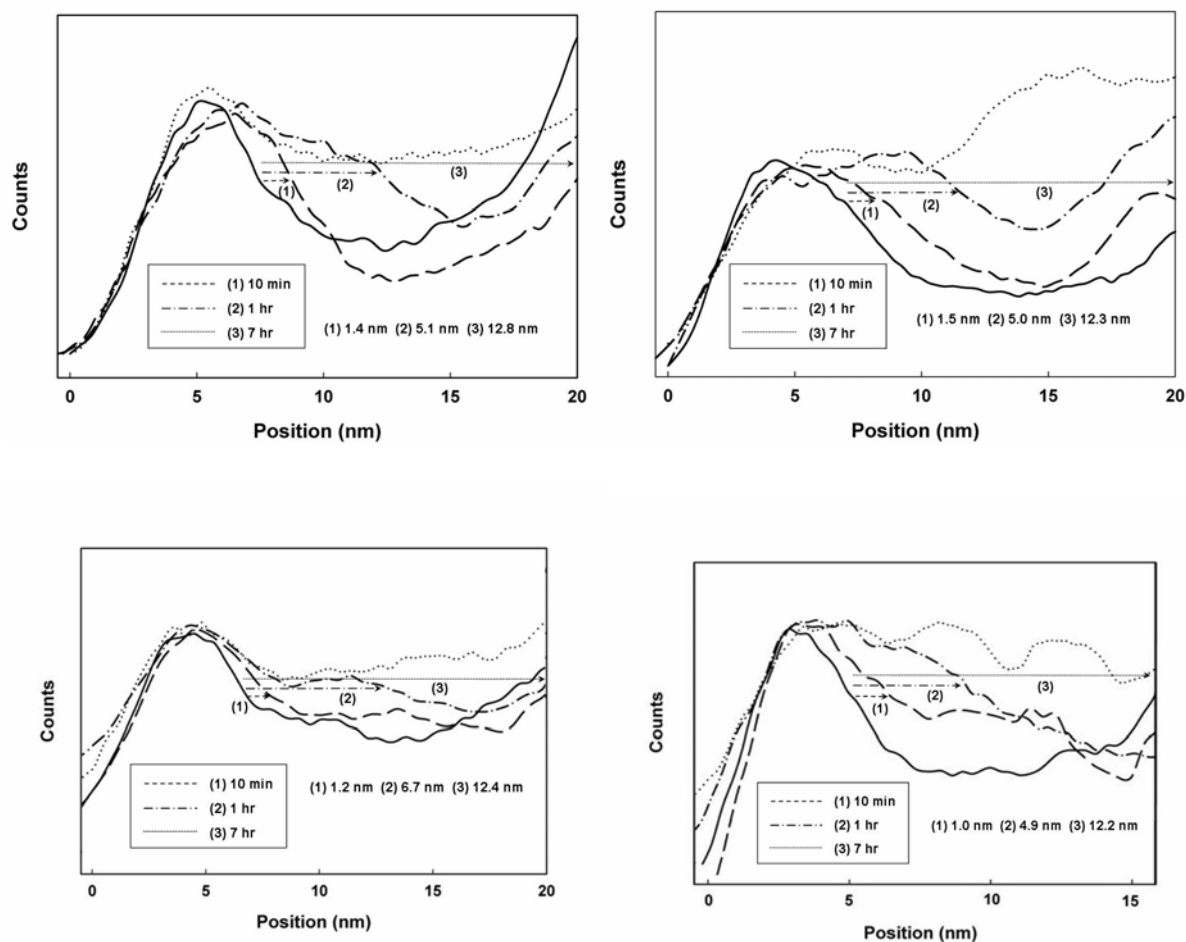


Figure S7. Nanobeam EDS maps of Te for four different nanorods after different aging times, illustrating how the diffusion lengths were determined. The average nanorod length decreased over time due to their coalescence, so the Te profiles are shown only at one end of the nanorods. However, to estimate the average diffusion length with aging time, both ends of the nanorods were examined. After 7 hr of aging, the Te and Se concentration profiles became uniform (with the exception of a small amount of residual Te deposition at the ends of the nanorods, as discussed in the main body of the paper) and the diffusion lengths were estimated as half the nanorod length.

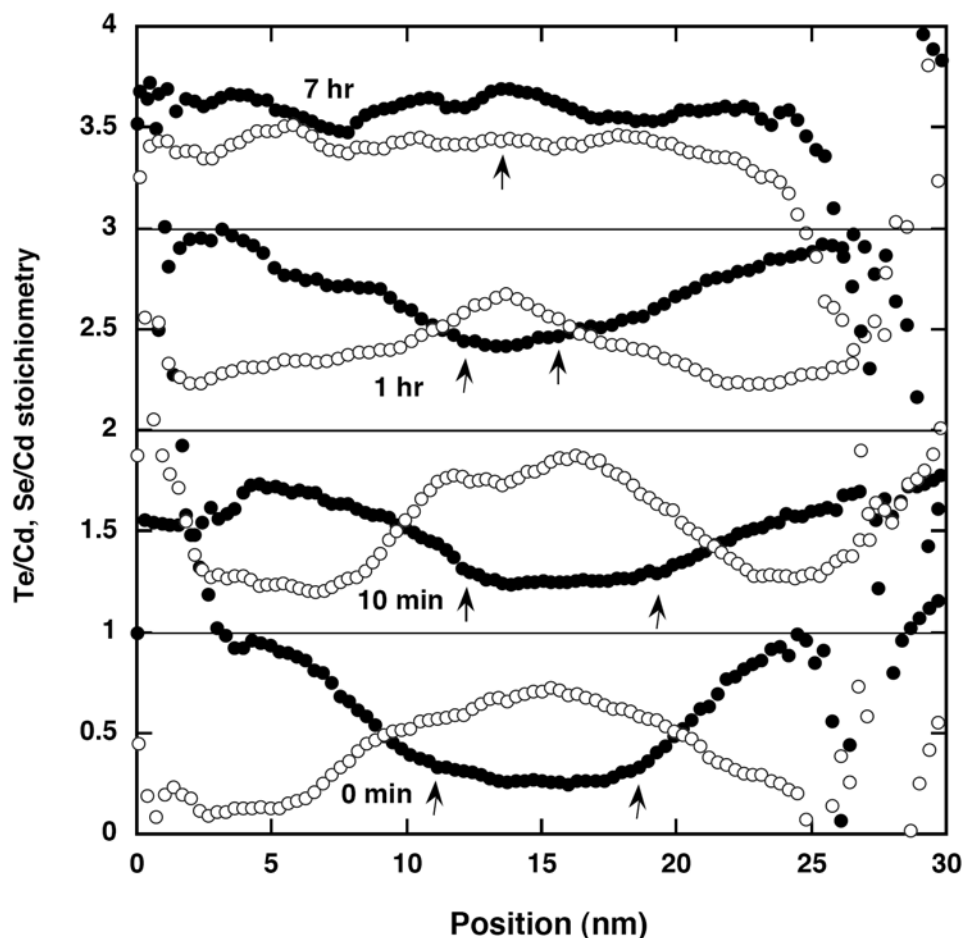


Figure S8. Te/Cd (●) and Se/Cd (○) stoichiometry determined from EDS mapping data as a function of position along the length of four nanorods isolated after the aging times indicated in the plot. The curves are offset in the vertical direction. The arrows indicate the Te edge in the nanorods. The Te present in the mid-section of the nanorods is the result of sidewall deposition, as discussed in the main text of the paper. After 7 hours of aging, the Te and Se compositions are uniform along the lengths of the nanorods with a slight excess of Te relative to Se, which is consistent with XRD data and results from continued Te deposition from residual reactant as the nanorods are aged in solution. Note that the compositions at the ends of the nanorods exhibit a significant amount of scatter and in some cases deviate above 1 or below 0 as a result of the relatively small measurement signals as the diameter narrows abruptly at the ends of the nanorods.

Evidence of strain at the CdTe/CdSe interface.

Figure S9 shows high resolution TEM images of a CdTe/CdSe/CdTe nanorod and FFTs taken at different positions along the nanorod. The crystal structure of the tips of the nanorod matches CdTe, whereas the center of the nanorod matches CdSe. At the interface between the CdTe ends and the CdSe cores, the lattice spacing gradually changes from CdTe to CdSe and there is no sign of a dislocation at the heterojunction.

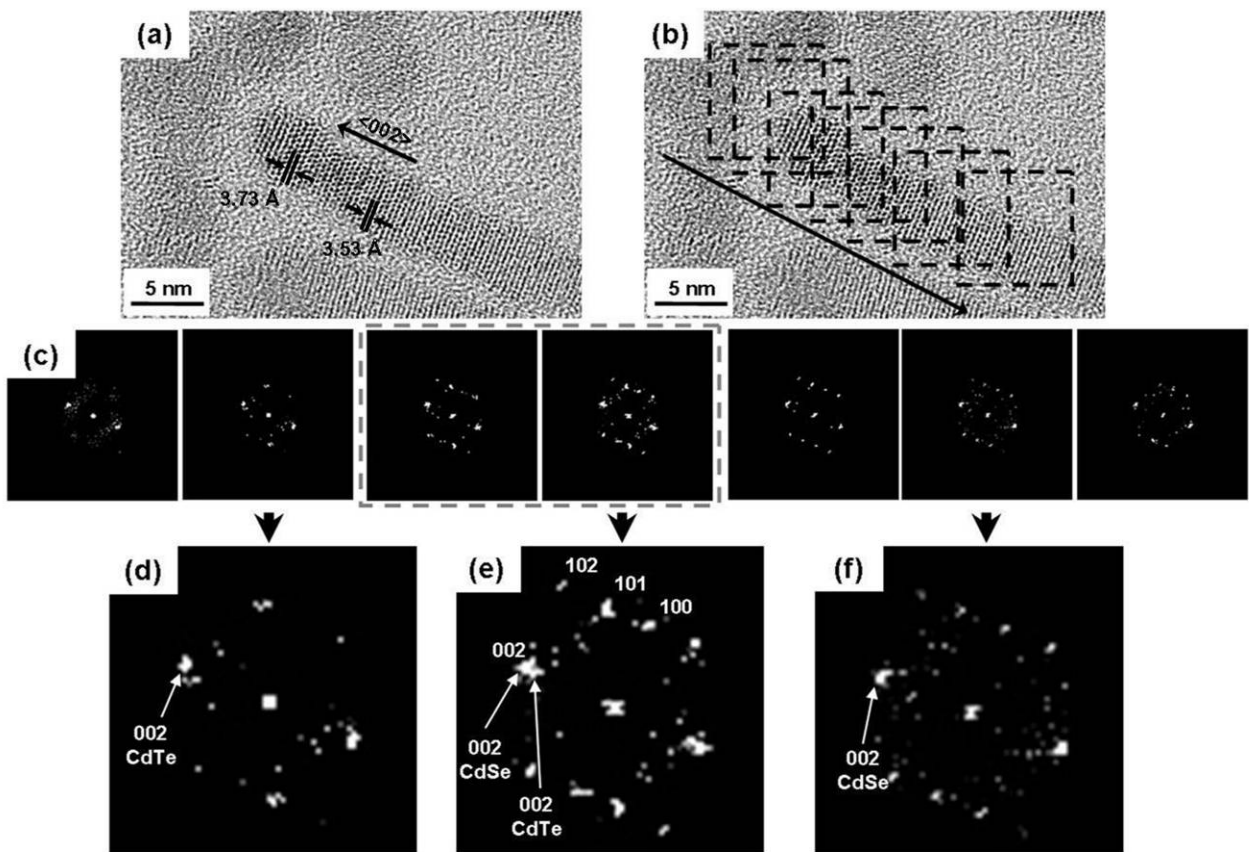


Figure S9. (a) High-resolution TEM image of a CdTe/CdSe/CdTe heterojunction nanorod. (c) FFTs of the regions of the nanorod outlined by the squares in (b) from top left to bottom right. The zone axis in (b) is $[2110]$. The nanorod is elongated in the $[002]$ direction. (d)-(f) Higher magnification of the second, fourth, and sixth FFTs in (c). (d) and (f) match the expected diffraction patterns for CdTe and CdSe, respectively, and the diffraction spots in (e) are slightly broadened compared to a pure sum of spots of CdTe and CdSe, indicative of the existence of different lattice spacings made by strain at the interface.

References

- (1) Peng, Z. A.; Peng, X. *J. Am. Chem. Soc.* **2002**, *124*, 3343.
- (2) Shieh, F.; Saunders, A. E.; Korgel, B. A. *J. Phys. Chem. B.* **2005**, *109*, 8538.
- (3) The derivation of the coalescence rate follows from Hawa and Zachariah,⁴ but there is a sign error in their derivation, so it is rewritten here.
- (4) Hawa, T.; Zachariah, M. R. *Phys. Rev. B* **2007**, *76*, 054109.
- (5) Batchelor, G. K., *An Introduction to Fluid Dynamics*, University Press: Cambridge, 1967.
- (6) Eyring, H. *J. Chem. Phys.* **1936**, *4*, 283-291.
- (7) Herring, C. *J. Appl. Phys.* **1950**, *21*, 437-445.